PHYSCIAL REVIEW VOLUME 1, NUMBER 1 5 JANUARY 1970

Ion-Ion Mutual Neutralization Cross Sections Measured by a Superimposed Beam Technique*

William H. Aberth and James R. Peterson
Stanford Research Institute, Menlo Park, California 94025
(Received 24 July 1969)

Ion-ion neutralization cross sections have been measured for $N^+ + O^-$, $N_2^+ + O_2^-$, and $O_2^+ + O_2^-$. The kinetic energy range, in the barycentric coordinate system covered by the experiment, is between 0.1 and 98 eV with an energy resolution of about 0.1 eV. The products of the neutralization cross section Q times the relative speed v_r are nearly independent of energy, having values close to 10^{-7} cm^3/sec for all three systems studied, except that below 0.5 eV the $N^+ + O^-$ and $N_2^+ + O_2^-$ systems show a rapid increase of Qv_r with decreasing energy. The experiment employs the superposition of positive- and negative-ion beams of several keV energy over a common path length of 33 cm. The beams are subsequently separated and the neutral products of the reaction are measured.

I. INTRODUCTION

In recent years, substantial progress has been made in the solution of the complicated problems related to the behavior of the earth's ionized layers. Laboratory measurements of some individual rate constants and cross sections have been made, and data on bulk behavior have been deduced from ionospheric measurements made under natural and disturbed conditions. This information has led to the development of complex ionospheric models.[1,2] Nevertheless, substantial gaps remain in our knowledge of important reaction rates for several classes of reactions for which satisfactory experimental techniques have not been developed yet and for which present theoretical approaches are still relatively crude. One of these classes is ion-ion mutual neutralization $A^+ + B^- \rightarrow A + B$, which is an important mechanism in the final neutralization of charge in the D region.[1,2]

Laboratory measurements of ion-ion neutralization have been made for only a few species, and until recently the techniques were restricted to bulk measurements on gases excited by rf discharges,[3] flames,[4] photons,[5] and electron beams.[6] Since these techniques involve a thermal distribution of interaction energies whose mean cannot be easily varied, and since there is no satisfactory control over the species and relative population of the interacting ions (in only one of the experiments were the ions identified by mass analysis), the interpretation of the data is seldom definitive. The method of superimposed or merged beams, however, does facilitate measurements with relative energies from above 100 down to 0.1 eV with reactants whose identities have been predetermined by mass analysis. This method, studied early by Cook and Ablow,[7] has been developed and put into effect in several laboratories to measure ion-neutral[8–10] and neutral-neutral[11] reactions. Initial results of the first direct ion-ion neutralization cross-section measurements on $N^+ + O^-$ have already been reported.[12] This paper is concerned with further work on the $N_2^+ + O_2^-$ and $O_2^+ + O_2^-$ systems in the barycentric energy range between 0.1 and 100 eV, as well as a detailed description of the apparatus and measurement technique.

II. EXPERIMENTAL DETAILS

The merged beam technique[7,8] involves superimposing particle beams of different speeds and observing their interactions over a known path length. In the present apparatus, the positive- and negative-ion beams are deflected in a magnetic field (see Figs. 1 and 2). Both beams have kiloelectron-volt energies in the laboratory coordinate system, but can have relative energies as low as 0.1 eV while merged. After traveling together for 33 cm, the beams are separated by electrostatic deflection and collected in two Faraday cups. The neutral particles formed by ion-ion neutralization, as well as a much larger "background" of neutrals formed by electron stripping and capture reactions of the beam ions with the ambient gas, continue along the superimposed beam direction. The neutrals are detected indirectly by the secondary-electron-emission current produced when they collide with a stainless-steel surface. The component of this current due to ion-ion neutralization is separated from the large background by a beam-chopping technique discussed below.

The vacuum envelope is fabricated from aluminum except for the bakeable interaction chamber, which is made of 304 stainless steel. The entire system is pumped by means of six nominal 6-in.

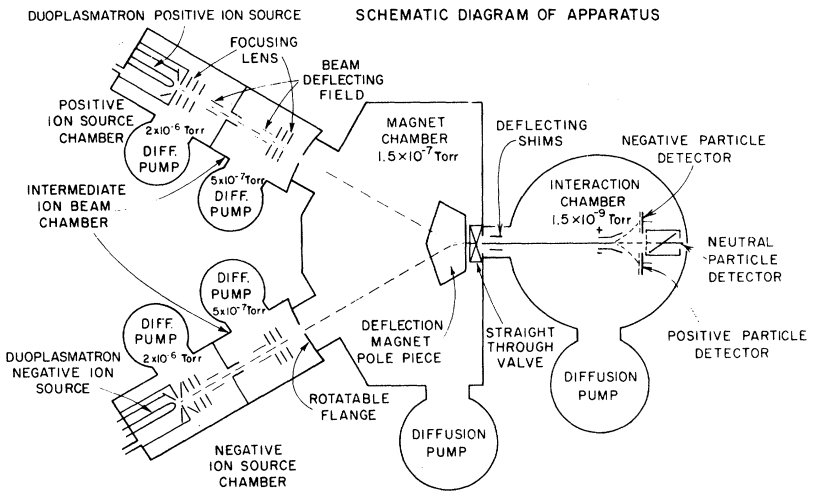

FIG. 1. Schematic of the merged-beam apparatus.

Clark DPD oil-diffusion pumps with a rated pumping speed of 1800 l/sec each. Dow Corning DC 705 diffusion-pump oil is used exclusively. The four diffusion pumps on the source and intermediate chambers utilize refrigerated "chevron"type baffles between the pumps and the vacuum system. The magnet and interaction chambers are each equipped with a trap that can be cooled either by liquid nitrogen or refrigerated Freon. After a period of operation, it was found that a sufficiently high vacuum ($\sim 1\times10^{-7}$ Torr) could be maintained by exclusively using the simpler Freon refrigeration. In order to obtain a pressure of 10^{-9} Torr in the interaction chamber, additional getter pumping and bakeout of the chamber were required. Titanium getter pumping was performed in the baffled upper-half of the interaction chamber by means of four 2-mm-diam filaments approximately 15 cm long, composed of a 15% molybdenum, 85% titanium alloy. A current of about 50 A through one filament for 2 min was sufficient to maintain a pressure of less than 2×10^{-9} Torr for about 2 h. Each filament is capable of about 2 h of continuous gettering, and the set of four filaments has been sufficient for more than six months of operation without replacement. Two 2-mm-diam tungsten filaments 20 cm long, mounted on the same flange as the getter filaments, were used to obtain a mild 150 °C bakeout of the interaction chamber. This was done by passing 170 A at 7 V through the parallel-connected tungsten filaments for a period of about 24 h.

The positive- and negative-ion beams are produced by duoplasmatron-ion sources of identical design. The sources were designed specifically for the present experiment and have been described in detail elsewhere.[13] The operation of both sources is identical except that the positive source has a 0.018-cm-diam extraction anode placed in line with the z electrode while the negative source has a 0.050-cm-diam extraction anode and the z electrode is placed about 0.090 cm off-axis. The negative-ion-source conditions differ from the positive-source conditions because of the beam-loading effect of the electrons, which is greatly reduced by the offset of the arc axis. In practice it was found that the oxide-coated cathode filaments exuded copious quantities of impurity gases, producing a large background of O^+, O_2^+, and OH^- ion beams which were not sufficiently resolved from the N^+, N_2^+, and O^- beams. In order to reduce the background pressure in the source region, a series of four 0.10-cm holes was drilled around the anode aperture, increasing the pumping speed from the arc region by a factor of 10, and consequently reducing the background ion beams by a similar factor.

The positive- and negative-ion beams are merged by means of an electromagnet placed entirely in the magnet chamber. The magnet is watercooled, and both of its coils are potted in high-temperature epoxy. The magnet is capable of producing a field of 7700 G in its 1.6-cm gap with a power expenditure of 90 W.

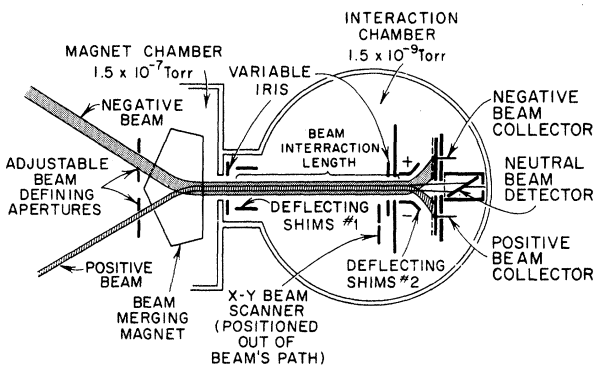

FIG. 2. Detailed schematic of the beam-merging and interaction regions.

In order to check the superposition of the positive- and negative-ion beams and to measure the cross-sectional intensity distribution of the beams, an X-Y scanner was installed in the interaction chamber. The scanner (see Fig. 2) consisted of a 1-mm-diam aperture in a stainless-steel plate that could be moved horizontally by means of a push-pull bellows feedthrough, or vertically by means of a rack and pinion device connected with a rotary feedthrough. A typical cross-sectional scan (horizontal) of the ion beams is shown in Fig. 3.

Since the fast neutral flux produced by the interaction of the ion beams with the background gas is more than two orders of magnitude greater than that produced by positive-ion–negative-ion neutralization, some means must be employed to separate these two components. The technique chosen is illustrated in Fig. 4. The negative and positive beams are electronically chopped at 800 and 1000 cps, respectively, and the 200-cps beat component of the neutral signal is then amplified by a PAR HR-8 narrow-band phase-sensitive amplifier. This signal, representing the product of the two ion beams, is proportional to the product of the neutralization cross section Q and the relative speed v. The determination of the proportionality factor is described in Sec. III.

III. PROCEDURE

The barycentric energy W of the positive- and negative-beam ions is obtained from the equation

$$W=\mu[(E^{+}/M^{+})^{1/2}-(E^{-}/M^{-})^{1/2}]^{2}+0.1\ \text{eV}\ . \quad (1)$$

Here E^{+} and E^{-} refer to the energies in eV in the laboratory coordinate system, M^{+} and M^{-} are the atomic masses of the positive- and negative-beam particles (amu), and μ is the reduced mass. The value of 0.1 eV added to the right-hand side of Eq. (1) is an estimate of the maximum increase

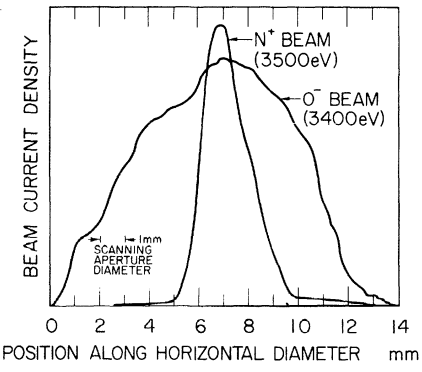

FIG. 3. Cross-sectional scan of the merged ion beams.

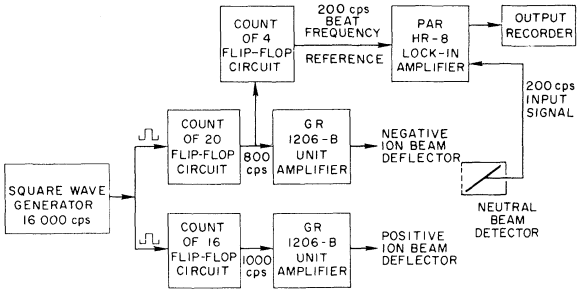

FIG. 4. Block diagram of the detection technique and circuitry.

in the barycentric energy due to imperfect collimation and internal beam divergence of the superimposed beams, and is obtained from the relationship[8] (for equal mass particles)

$$\Delta W<0.54Ed^{2}/8L^{2}\ , \quad (2)$$

where ΔW represents the increase in average barycentric energy due to the beam divergence, $E=\frac{1}{2}(E^{+}+E^{-})$, d is the width of the ion beams, and L is the distance between the collimating apertures. In the present experiment, $E\sim3000$ eV, $e=0.8$ cm, and $L=33$ cm. For the special case of equal positive- and negative-ion masses and where the difference energy $\Delta E=E^{+}-E^{-}$ is small compared to E^{+} or E^{-}, then Eq. (1) reduces to the approximation

$$W=\Delta E^{2}/8E\ . \quad (3)$$

It can be shown from Eq. (3) that the kinetic-energy spreads of about 3 eV (full width at half-maximum) in the laboratory coordinate system of both the positive- and negative-duoplasmatron-ion sources will produce a negligible energy spread in the c. m. system when the average laboratory beam energy is several keV. This will hold true even when the positive- and negative-ion masses differ by a small amount.

The rate at which the positive ions B^{+} are neutralized by C^{-} ions via two-body ion-ion neutralization is given by

$$d[B^{+}]/dt=-\alpha[B^{+}][C^{-}]\ . \quad (4)$$

Here α is the rate coefficient of the reaction and in thermal gases represents an average value of Qv_{γ}, where Q is the cross section and v_{γ} the relative speed, the average being taken over the relative thermal-velocity distributions of the particles. In the present experiment, however, the spread in v_{γ} is relatively very small, and α can be expressed as

$$\alpha=Qv_{\gamma}\ . \quad (5)$$

In terms of observed experimental parameters, Eq. (4) can be restated as

$$d[B^+]/dt = -I_0/2\gamma e \ . \tag{6}$$

The left-hand side is equivalent to half the total number of neutrals produced per unit time. I_0 is the total neutral detector current, γ is the effective neutral-particle secondary electron-emission coefficient, and e is the electronic charge. The experimental determination of γ is explained below. Assuming B^+ and C^- are both traveling in the z direction with respective currents I^+ and I^-, current densities J^+ and J^-, and velocities v^+ and v^- in the laboratory coordinate system; then the particle densities of the positive- and negative-ion beams in the volume $dV = dAdz$ are J^+/ev^+ and J^-/ev^-. Equation (4) can now be rewritten as

$$-I_0/2\gamma e = -(Qv_r/e^2v^+v^-)\int J^+J^-dV \ . \tag{7}$$

J^+ and J^- are assumed to be independent of the z coordinate in the interaction volume v. The experimental procedure is to broaden one beam (the negative, for example) relative to the other (see Fig. 3) to such an extent that the density of the broadened beam is relatively constant over the region of the narrower beam. Under these conditions, the value of J^- is constant over the region of integration and may be taken outside the integral. If A is a common area through which most of I^+ passes, and where J^- is constant, then we can write

$$J^- = I_A^-/A \ , \tag{8}$$

where I_A^- is defined as the total current (negative) passing through A. Equation (7) can now be written

$$I_0/2\gamma e = Qv_r I_A^- (e^2v^+v^-A)^{-1}\int J^+dV \ . \tag{9}$$

The value of the integral in Eq. (9) is simply the total positive-beam current I^+ times the interaction length L, and hence, we obtain finally

$$Qv_r = I_0 eAv^+v^-(2I^+I_A^-L\gamma)^{-1} \ . \tag{10}$$

It is now necessary to take into account in Eq. (10) the effects of chopping both beams and the amplification factor of the lock-in amplifier. If i^+ and i_A^- represent the half-amplitudes of the square-wave chopped-beam currents (thus, the average dc value), then the actual values of the time-dependent currents $I^+(t)$ and $I_A^-(t)$ can be expanded in Fourier series as

$$\begin{aligned} I^+(t) &= i^+[1+(4/\pi)\cos\omega t - \tfrac{1}{3}\cos 3\omega t + \cdots] \ , \\ I_A^-(t) &= i_A^-[1+(4/\pi)\cos(\omega' t) - \tfrac{1}{3}\cos 3(\omega' t) + \cdots] . \end{aligned} \tag{11}$$

[We have arbitrarily set the constant phase difference (at $t=0$) between the two chopping signals equal to zero. This is a trivial simplification.] The time-dependent product $I^+I_A^-$ which enters Eq. (10) is

$$I^+I_A^-(t) = i^+i_A^-[1+(4/\pi)(\cos\omega t+\cos\omega' t) + \cdots + (16/\pi)\cos\omega t\cos\omega' t + \cdots] . \tag{12}$$

Expanding $\cos\omega t\cos\omega' t$ and keeping the lowest frequency component yields

$$I^+I_A^-(t) = (8i^+i_A^-/\pi^2)\cos(\omega-\omega')t + \cdots \ . \tag{13}$$

The Fourier component of the resultant neutral detector current, I_Q, at this frequency I_0 is

$$I_0(t) = KI^+I_A^-(t) = (K8i^+i_A^-/\pi^2)\cos(\omega-\omega')t \ , \tag{14}$$

where K, obtained from Eq. (10), is

$$K = 2Qv_r L\gamma/eAv^+v^- \ . \tag{15}$$

Finally, I_0', the rms value of $I_0(t)$, which is measured by the lock-in-amplifier, is

$$I_0' = (4\sqrt{2}/\pi^2)Ki^+i_A^- \ , \tag{16}$$

and solving for Qv_r from Eqs. (15) and (16) yields

$$Qv_r = (\pi^2 I_0' Av^+v^-e)/(8\sqrt{2}\, i^+i_A^-\gamma L) \ . \tag{17}$$

A more practical arrangement of Eq. (17) is

$$Qv_r = 2.69\times10^{-7}AI_0'(\gamma Li^+i_A^-)^{-1} \times (E^+E^-/M^+M^-)^{1/2}\,\mathrm{cm^3\,sec^{-1}} \ , \tag{18}$$

where E^+, E^- and M^+, M^- are defined as in Eq. (1), i^+ and i_A^- are in amperes, A is in cm^2, and L is in cm. In practice, A is defined by the area of the first variable iris at the entrance to the interaction chamber (see Fig. 2) stopped down to 0.32 cm in diam. This aperture is used to measure the current density of the broadly focused beam. (The second variable iris is normally kept fully open to 1.58 cm in diam except during beam alignment.) The narrower ion beam current (I^+ here) is measured with both variable irises fully open. In general, the ratio of the broader beam current, with the first iris fully open, to its value with the iris stopped down to 0.32 cm in diam is about 5, while that of the narrower beam is less than 2.

The value of γ in Eq. (18) is taken as the average of the secondary electron-emission coefficients of the positive and negative beams. This approximation is an important simplification, since an exact measurement is exceedingly difficult. It appears

justified since, for beam energies of this experiment (2.5–4.6 keV), γ is found to change only slightly for different charge states of the particle.[14] Our experience with beams of H^+, H^-; O^+, O^-; and O_2^+, O_2^- indicates that the secondary electron-emission coefficient for the negative beam is greater than the positive beam of the same species by only 10–30% between 2.5–4.6 keV. In practice, γ is measured after every two or three data points are taken, to reduce effects due to changing surface conditions of the neutral detector and changing energies of the ion beams.

A small pressure-dependent component of the ion-ion neutralization signal persists in all measurements. This is due to space-charge modulation of one ion beam by the other producing a beam-frequency perturbation of the direction of motion of both ion beams. Subsequent charge exchange of either ion beam with the background gas produces a similar perturbation in the neutral background signal. If the merged-beam defining apertures and neutral-particle detecting surface are all large and the neutral-particle detection efficiency is constant over the detector's surface, then this perturbation will not register as a neutralization signal, since there is no modulation of the total neutral-particle flux. These ideal conditions do not exist in practice. The magnitude of this spurious signal varies between a negligible amount and 25% of the neutralization signal at background pressures between 1 and 2×10^{-9} Torr and is dependent on the degree of beam alignments and focusing. The pressure-dependent component of the neutralization signal, therefore, is a sensitive indicator of the beam alignment and focusing conditions. By doubling the background pressure during each measurement with the use of a variable leak valve, the unwanted signal component (which is proportional to background pressure) can be measured and subtracted out.

Initially, the beam interaction path extended from the downstream edge of the merging magnetic field to the terminal deflectors in front of the detector. However, systematic neutralization-signal errors were found to originate from pressure modulations in the magnet region, apparently caused by those extraneous ions in the initial (unfiltered) beams as they struck the chamber walls after being deflected out of the beams by the magnet. To eliminate this error, a pair of deflecting shims (No. 1 in Fig. 2) were installed just inside the interaction chamber. These deflectors become the effective upstream terminus of the interaction path. The change in neutral signal caused by placing a deflecting voltage on shims No. 1 was accepted as the true ion-ion neutralization component (after the pressure-dependent component was subtracted out). This procedure therefore eliminated any systematic effects from the magnet region up to the deflecting shims and also helped to define the interaction length L. For the species measured, the background signal arising from the magnet region amounted to less than 30% of the total neutral signal and was easily subtracted out by the above procedure.

In addition to its beneficial roles as mass-separator and beam-merger, the magnet also acts as an undesirable astigmatic lens in the ion optical system. Uncorrected, this lens distorts each beam so that its cross section departs from axial symmetry and becomes a narrow ellipse by the time it enters the aperture in front of the neutral detector. There are two consequences: (a) The beams do not overlap properly over the interaction path, and (b) because of their asymmetry, the beams are usually partially intersected by the edge of the aperture located in front of the detector, and a small space-charge modulation in the beam profile yields an interference signal at the beat frequency. To correct the magnet's astigmatism, a simple electrostatic lens was constructed for each beam and placed inside the magnet just behind the movable apertures. These lenses produced focusing only in the direction parallel to the magnetic field, leaving ion velocities perpendicular to the field unaffected. The focusing voltages for these lenses are readjusted after each change in ion energy.

As an additional protection against possible beam instabilities, two 0.95-cm-diam beam apertures were placed immediately in front of the magnet pole pieces. These serve to confine the ion beams to the central region of the 1.58-cm magnet gap, thus preventing charging of the pole surfaces. Each aperture can be externally adjusted for changes in beam approach angle.

IV. RESULTS AND DISCUSSION

The results of the measurements of $N_2^+ + O_2^-$ and $O_2^+ + O_2^-$ are shown in Figs. 5 and 6. Figure 7 presents, for comparison, the $N^+ + O^-$ data of Ref. 12 (small energy corrections have been made to the original data for points with relative ener-

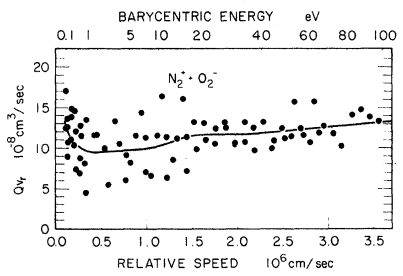

FIG. 5. Neutralization-rate measurements versus velocity for $N_2^+ + O_2^-$. The solid curve represents an approximate least-squares fit of the data points.

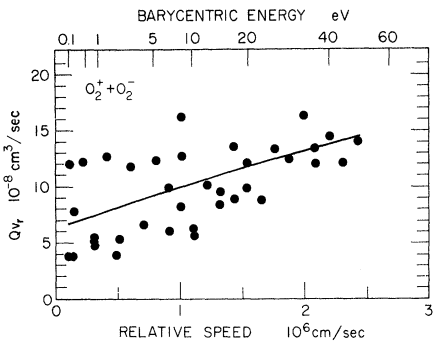

FIG. 6. Neutralization-rate measurements versus velocity for $O_2^+ + O_2^-$. The solid curve represents an average straight-line fit of the data points.

gies above 30 eV, and all cross sections have been increased by 11% to correct for a calibration error). The data have been plotted as the product Qv_γ, where Q is the neutralization cross section and v_γ is the relative speed of the interacting ions. It can immediately be seen that (i) the magnitude of Qv_γ is in the vicinity (within 50%) of 10^{-7} cm^3/sec for all reactants over the energy range 0.1–100 eV; (ii) Qv_γ is a fairly constant (or slowly changing) function of energy in this range, except that for $N^+ + O^-$ and $N_2^+ + O_2^-$ a rather sharp increase in Qv_γ occurs as the barycentric energy decreases below 0.5 eV. (A similar characteristic may be obscured in the $O_2^+ + O_2^-$ case, since these data display considerably more scatter than those of the other reactions.)

In Figs. 5 and 7 we have also plotted a least-squares computer fit of the data points to an 11th-deg polynomial. This procedure is a useful method of averaging the data points when they have an irregular statistical distribution along the abscissa. It was used especially to bring out any structural details at the low-energy end of the data where there appeared to be an abrupt change in the rate coefficient and where a greater number of data points were taken. An 11th-deg polynomial yielded a better fit to the data than did the lower-order polynomials that were tried. The computer curves showed small rather rapid oscillations toward the upper-energy ends due to lack of data beyond the last (high-energy) point as well as insufficient data for good statistics.[12,15] These oscillations were thus insignificant, and a smooth line was used for this portion instead of the computed curve. The curve in Fig. 6 represents a weighted-average straight-line fit to the data points. The standard deviations of the data from the plotted curves of $N^+ + O^-$, $N_2^+ + O_2^-$, and $O_2^+ + O_2^-$ are 1.6, 1.7, and 2.7×10^{-8} cm^3/sec, respectively.

Various sources contribute to the statistical cross-section uncertainty, and some systematic error may also be present. The assumption that γ is the average value of γ^+ and γ^-, as discussed in Sec. III, may introduce an error of 10–20%. Also, the estimated uncertainty in the secondary-electron-emission-coefficient measurement is ±10%. The electrometer measurements of B^+, C^-, and I_0' are good to within 5%. The measurement of A [see Eq. (18)] is accurate to only 20% owing to hysteresis present in the variable-iris mechanism. Probably a major part of the scatter in the data points is due to beam alignment and focusing problems. The assumption that one of the ion beams is broad and has a constant density while the other is extremely narrow is only a first approximation to the actual conditions (see Fig. 3). The routine determinations of the beam-density distributions, which are made for each data point to test the validity of this assumption, are obtained (using a variable iris) at only one position along the merged-beam path. Since the alignment and shape of the two beams will vary over the entire interaction length, a further uncertainty is introduced. The over-all error caused by the beam-overlap problem is perhaps 30%. As the beams approach the same average laboratory velocity, the minimum average relative energy is attributed to beam divergence and is estimated to be 0.1 eV. Since it is in this low-energy range that the rate coefficient for $N^+ + O^-$ and $N_2^+ + O_2^-$ is increasing rapidly, it can be seen that uncertainty in the measurement will be larger in this region. The total error due to all of the above mentioned causes is probably less than 40%, except below 0.5-eV relative energy, where a somewhat larger error can be expected due to uncertainties in the relative velocity.

It should also be noted that there is an uncertainty in the state of excitation of the interacting beam ions. Studies of ion beams produced by electron bombardment indicate that as much as 35% of the O_2^+ beam created by 150-eV electrons may be in a metastable state,[16] and a smaller percentage of the N_2^+ beam may be excited. The effective electron energy in our ion-source arcs may be considerably lower than 150 eV, but, in any case, we have no knowledge of the state population. Also some

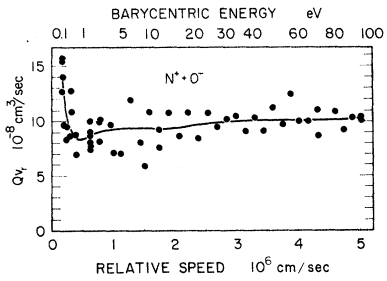

FIG. 7. Neutralization-rate measurements versus velocity for $N^+ + O^-$. The solid curve represents an approximate least-squares fit of the data points.

vibrational excitation of the O_2^- ion probably exists. How these energy states affect the neutralization rate is unknown. It is possible that the larger amount of scatter in the $O_2^+ + O_2^-$ data is attributable, in part, to this cause, since the ion-source operating conditions are not always the same. However, it is more likely that the scatter is due to the effects of instabilities on the overlap and alignment of the beams.

None of the reactions we have measured have been studied theoretically, although theoretical work has been done on $H^+ + H^-$ by Bates and Lewis,[17] $H^+ + Li^+$, Na^+, and K^+ by Bates and Boyd,[18] and $O^+ + O^-$ and $O^+ + O_2^-$ by Magee.[19] (Victor and Dalgarno are currently treating the $H^+ + H^-$ system[20] which has recently been studied experimentally at energies above 250 eV.[21]) The Landau-Zener approximation for the curve-crossing reaction mechanism has been used as the basis for most theoretical calculations to date. The calculation of $H^+ + H^-$ neutralization is the most rigorously studied, and a plot of the theoretical results of Bates and Lewis[17] for this species is shown in Fig. 8. The similarity between this curve and the experimental plot of $N_2^+ + O_2^-$ and $N^+ + O^-$ neutralization (Figs. 5 and 7) is apparent. The general characteristics of the Landau-Zener calculation are indicated in these curves – namely, that Qv becomes constant with increasing v, and that a sharp rise in Qv at low energies is produced by a $(1 + \Delta U/E)$ factor in the cross-section calculation, where ΔU represents the exothermic energy of the reaction. For the $H^+ + H^-$ reaction, ΔU is 2.65 or 0.76 eV for the two most likely final states, and for the $N^+ + O^-$ reaction, ΔU can vary from about 2.6 to 0 eV; hence one might begin to see the effects of the $\Delta U/E$ term below 2 eV. In the molecular case, there is the additional complication of vibrational and rotational energy levels, as well as the electronic levels, which may smear out or possibly move this structure toward lower relative energies where it is not experimentally observable. A comparison of the $N^+ + O^-$ and $N_2^+ + O_2^-$ neutralization-rate curves indicates that the low-energy structure is more suppressed in the molecular case.

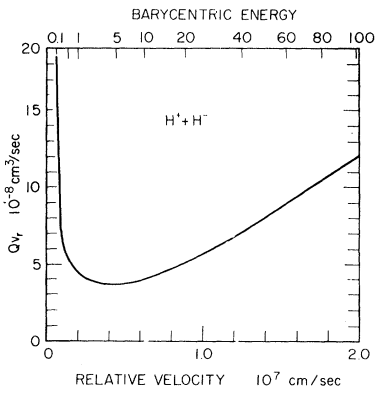

FIG. 8. Plot of the neutralization rate versus velocity for $H^+ + H^-$ based on the calculations of Bates and Lewis (see Ref. 17).

ACKNOWLEDGMENTS

The authors wish to thank George Conklin and Ralph Leon for their skillful and willing technical help throughout the course of this work. They are also grateful to Dr. C. J. Cook for his original conception of the technique and consistent support, and Dr. F. T. Smith and Dr. D. C. Lorents for many valuable discussions.

---

*Work sponsored by the Defense Atomic Support Agency Reaction Rate Program through contract with the Air Force Cambridge Research Laboratories.

[1]E. E. Ferguson, Rev. Geophys. 5, 305 (1967).

[2]R. E. LeLevier and L. M. Branscomb, J. Geophys. Res. 73, 27 (1968).

[3]T. Y. H. Young, Proc. Phys. Soc. (London) 71, 341 (1958).

[4]T. M. Sugden, Trans. Faraday Soc. 54, 372 (1958).

[5]B. H. Mahan and J. C. Person, J. Chem. Phys. 40, 392 (1964).

[6]M. N. Hirsh, G. M. Halpern, and N. S. Wolf, The G. C. Dewey Corporation, Report No. R-198-4, 1967 (unpublished).

[7]C. J. Cook and C. M. Ablow, Air Force Cambridge Research Commission Report No. TN-59-472, 1959 (unpublished).

[8]S. M. Trujillo, R. H. Neynaber, and E. W. Rothe, Rev. Sci. Instr. 37, 1655 (1966).

[9]R. H. Neynaber, S. M. Trujillo, and E. W. Rothe, Phys. Rev. 157, 101 (1967).

[10]V. A. Belyaev, B. G. Brezhnev, and E. M. Erastov, Zh. Eksperim. i Teor. Fiz. 55, 1170 (1967) [English transl.: Soviet Phys. – JETP 25, 777 (1967)].

[11]R. Neynaber, P. K. Rol, and E. A. Entemann, Conference on Heavy Particle Collisions (Queens University Press, Belfast, Ireland, 1968).

[12]W. Aberth, J. R. Peterson, D. C. Lorents, and C. J. Cook, Phys. Rev. Letters 20, 979 (1968).

[13]W. Aberth and J. R. Peterson, Rev. Sci. Instr. 38, 745 (1967).

[14]H. C. Hayden and N. G. Utterback, Phys. Rev. 135, A1575 (1964); E. S. Chambers, *ibid.* 133, A1202 (1964); V. G. Tel'kovskii, Dokl. Akad. Nauk. SSSR 108, 444 (1956) [English transl.: Soviet Phys. – Doklady 1, 334 (1956)].

[15]S. Margulies, Rev. Sci. Instr. 39, 478 (1968).

[16]B. R. Turner, R. F. Mathis, and J. A. Rutherford,

Conference on Heavy Particle Collisions (Queens University Press, Belfast, Ireland, 1968), p. 126.
[17]D. R. Bates and J. T. Lewis, Proc. Phys. Soc. (London) A68, 173 (1955).
[18]D. R. Bates and T. J. M. Boyd, Proc. Phys. Soc. (London) A69, 910 (1956).
[19]J. L. Magee, Discussions Faraday Soc. 12, 33 (1952).
[20]G. A. Victor and A. Dalgarno (private communication).
[21]R. D. Rundel, K. L. Aitken, and M. F. A. Harrison (to be published).